Frequency Control in an Isolated Power System with High Renewable Energy Penetration

Ben Ivory
School of Engineering
University of Tasmania
Hobart, Australia
bivory@utas.edu.au

Evgenii Semshchikov
School of Engineering
University of Tasmania
Hobart, Australia
evgenii.semshchikov@utas.edu.au

Michael Negnevitsky
School of Engineering
University of Tasmania
Hobart, Australia
michael.negnevitsky@utas.edu.au

Abstract— **Isolated power systems have traditionally used diesel generation to ensure reliable and stable power. Due to the high costs of purchasing and transporting diesel fuel to remote areas, these communities have been integrating renewable energy sources such as wind and solar to reduce reliance on diesel and decrease operating costs. When there is enough renewable energy to supply the load diesel engines can be turned off completely. This decreases fuel consumption but introduces stability problems due to the lack of spinning reserves and inertia. Energy storage systems can be used effectively for frequency control but are still very expensive. Therefore, some isolated power systems will limit the acceptance of renewables in order to keep diesel engines online for frequency control. This paper investigates the use of a dump load and enhanced frequency response techniques for wind turbines as methods for frequency control to facilitate 100% acceptance of renewable energy. Results showed that a dump load was sufficient for frequency control and kept frequency within 0.3 Hz of nominal frequency. Advanced wind turbine control systems were found to only slightly improve the frequency response by 0.03 Hz.**

I. INTRODUCTION

Communities located in remote areas or islands are usually supplied by power systems separated from the main grid. Traditionally power in these isolated power systems (IPSs) are provided by diesel generation which also ensures the reliability and stability of the power system [1]. However, the operating cost of diesel generation is high and transporting the diesel fuel to the communities is expensive. Diesel is also a major contributor to greenhouse gas emissions. Therefore IPSs have been steadily integrating renewable energy (RE) to reduce dependence on diesel and decrease both costs and emissions [2]. A small investment can have a significant impact and some IPSs have achieved annual renewable energy penetration of over 50% and at times an instantaneous penetration of 100% operating without diesel generation (zero diesel operation).

The most widely available and abundant renewable energy sources (RES) are heavily reliant on environmental factors which are stochastic and intermittent. RE generation is constantly changing and rarely matches the instantaneous power demand. Mismatch between power generation and demand causes the system frequency to deviate. In conventional power systems the inertia from synchronous generators limits the rate of change of frequency (ROCOF) and output of the generators is changed to restore the frequency. With RES replacing conventional generation the overall system inertia is decreased [3] and results in increased ROCOF and larger frequency excursions [4]. This is especially true for isolated power systems which already have limited inertia [5]. As a consequence, high penetrations of

renewable energy introduce stability and reliability problems into the power system. Some IPSs limit the acceptance of renewables to avoid these issues, which leads to an increase in curtailed renewable energy and discourages further renewable energy integration [6]. Enabling technologies must be implemented in order to support 100% acceptance of renewables.

One solution is to use energy storage systems (ESS) in IPSs with high RE penetration. Batteries [7], supercapacitors [8], and flywheels [9] have a fast response time and are suited for improving power quality and providing primary frequency control. Capacity-orientated ESS such as pumped-hydro storage [10] and hydrogen storage [11] are suitable for long-term storage and balancing slowly varying loads. Different kinds of ESS can be used together to form a hybrid ESS. A common example is using a supercapacitor for balancing rapid power fluctuations while a battery is used only for slower power changes, extending the lifetime of the battery [12]. Despite advancements in ESS technology, there are still significant investments required that limit their widespread use and encourage consideration of alternatives.

Controllable loads are another way of supporting high penetration of RES. A dump load is a variable resistor which can be used to consume excess renewable energy. This method is cheaper than ESS but does not have any other benefits offered by ESS as the energy spillage is non-recoverable [13]. A different approach is to use demand response by controlling certain loads on the consumer side to decrease their power demand. This can extend zero diesel operation by providing spinning reserve when RE suddenly drops. This method is cost effective but requires interconnected communication networks [14].

Wind energy conversion systems (WECS) can be modified to support a grid with high RE penetration. Variable speed wind turbines are decoupled from the grid either partially or fully by power electronics, respectively providing limited or no inertial response [4]. The control system for the power electronics can be modified to implement frequency control in different ways. Inertial control creates virtual wind inertia by extracting the kinetic energy stored in the rotating masses of the wind turbine and releasing the energy into the grid when frequency drops [15]. However, this can generate a power dip directly after the energy release when the turbine accelerates back to operational speed potentially causing another frequency event [16]. Power reserve can be kept by purposefully operating the wind turbine away from its maximum power point (MPP) using suboptimal power point tracking to enhance its frequency control [16]. With power kept in reserve, a droop controller can adjust the power output

of the turbine to provide primary frequency response using pitch angle control [5] or rotor speed control [16].

It is clear that despite what technologies are used, diesel generation cannot yet be completely eliminated. However, with enabling technology it is possible to run IPSs with diesel generation shut down when an abundance of renewable energy is available. An example of this is the King Island IPS in Australia. It is able to run without diesel generation for up to 20% of the year [17]. However the system relies on a large battery ESS which is very costly.

This paper will explore the use of a dump load and frequency control from wind turbines to regulate the frequency of an IPS when running without diesel generation. The paper is structured as follows. Section 2 presents the simulation models of each generation element. Section 3 explains the control methods used during zero diesel operation. Case studies are discussed in Section 4. Section 5 concludes the paper.

II. GENERATION ELEMENTS

A. Synchronous Generator

The synchronous generator (SG) is modelled using the standard seventh order model [18]. The rotor has one field winding and three damping windings, notated as *fd*, *kd*, *kq1* and *kq2* respectively. The park transformation transforms the stationary stator variables to a reference frame known as the *dq*-axis rotating at the synchronous speed. The subscripts *d* and *q* refer to variables projected to the respective axis. Details of the equations used to model the SG can be found in [2]. The excitation system provides direct current to the field windings and can adjust this current to achieve the desired performance. The excitation system used is AC1A from [19].

The conventional diesel engine transient response is simulated with a governor and engine model shown in Fig. 1. The governor detects frequency deviation and instructs the actuator to adjust the fuel flow rate. The delay represents the time needed to produce the torque after fuel has been injected [2]. The governor model and parameters were obtained from [20].
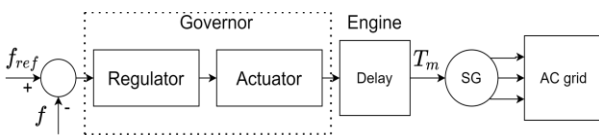

Fig. 1.   Conventional diesel engine model

B. Photovoltaic Array

Photovoltaic (PV) arrays convert solar irradiance to DC current. The most common way to model a PV array is by using the practical single diode model [21]. The model takes solar irradiance, cell temperature and network voltage as inputs and calculates the current flowing to the grid. The model is based on the equations provided in [22]. The output current of the PV array is

$$I_{PV} = N_p I_{ph} - N_p I_d - \frac{V_d}{R_p \frac{N_s}{N_p}} \tag{1}$$

where I_{PV} is the output current, N_s is the number of modules in series, N_p is the number of modules in parallel, I_{ph} is the photocurrent, I_d is the diode current, V_d is the diode voltage and R_p is the parallel resistance of a single module.

The diode voltage is

$$V_d = V_{PV} + I_{PV} R_s \frac{N_s}{N_p} \tag{2}$$

where V_{PV} is the output voltage of the PV array and R_s is the series resistance of a single module.

The photocurrent is

$$I_{ph} = \frac{G}{G_{ref}} (I_{sc} + K_i (T_c - T_r)) \tag{3}$$

where G is the solar irradiance, G_{ref} is the reference solar irradiance, I_{sc} is the short circuit current of the module, K_i is the current temperature coefficient, T_c is the cell temperature and T_r is the reference temperature.

The diode current is

$$I_d = I_s \left(\exp\left(\frac{qV_d}{N_s N_c K A T_c} \right) - 1 \right) \tag{4}$$

where I_s is the saturation current, q is the charge of an electron, N_c is the number of cells in the module, K is the Boltzmann constant and A is the ideality factor of the diode.

The saturation current is

$$I_s = I_{rs} \left(\frac{T_c}{T_r} \right)^3 \exp\left[\left(\frac{qE_g}{AK} \right) \left(\frac{1}{T_r} - \frac{1}{T_c} \right) \right] \tag{5}$$

where I_{rs} is the reverse saturation current and E_g is the energy band gap.

The reverse saturation current is

$$I_{rs} = \frac{I_{sc}}{\exp\left(\frac{qV_{oc}}{N_s N_c K A T_c} \right) - 1} \tag{6}$$

where V_{oc} is the open circuit voltage.

The PV array configuration is shown in Fig. 2. The PV array is connected to a DC/AC converter controlled using maximum power point tracking (MPPT). The output is filtered using an RLC filter before the grid connection point. Control uses the DC and AC currents and voltages to determine the PWM signals sent to the inverter.
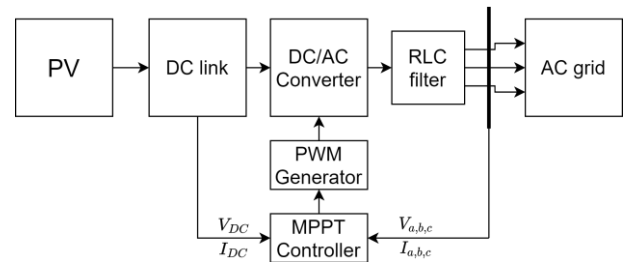

Fig. 2.   PV array connected to the grid

C. Wind Turbine

The amount of power produced by a wind turbine is

$$P_m = c_p(\lambda, \beta) \frac{\rho A}{2} v_{wind}^3 \qquad (7)$$

where c_p is the power coefficient, λ is the tip speed ratio, β is the pitch angle, ρ is the density of air, A is the area swept by the rotor blades and v_{wind} is the speed of the wind. The wind turbine rotor is mechanically coupled to a doubly fed induction generator (DFIG). The DFIG is modelled using the standard fourth order model. Details of the equations used to model the DFIG can be found in [2].

The wind energy conversion system (WECS) is shown in Fig. 3. The stator windings of the DFIG are connected directly to the grid. The rotor windings are connected to the grid through back-to-back PWM converters. This allows the rotor to rotate at any angular velocity while also reducing the size of the power converters compared to other variable speed wind turbine configurations.
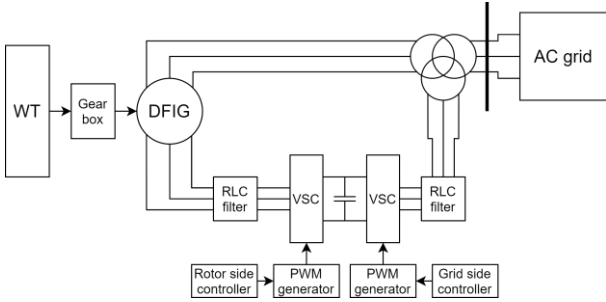

Fig. 3.   WECS connected to the grid

III. FREQUENCY CONTROL METHODS

A. Dump Load

The dump load is a variable resistor used to curtail excess energy generated by RES. This enables the power system to operate under conditions when renewable energy is greater than demand and helps to keep load balanced with generation. In MATLAB the dump load can be modelled as a controllable current source. A PI controller is used to take in the frequency error and adjust the dump load accordingly. The control signal is limited to positive values as a dump load cannot generate power. See Fig. 4 for the control system.
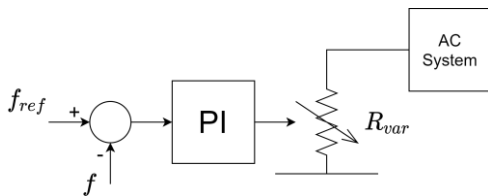

Fig. 4.   Controller for the dump load

B. Suboptimal Power Point Tracking

It is common for wind turbines to use some form of MPPT in order to extract maximum power from the wind. By purposefully operating the wind turbine away from the maximum power point (MPP), power can be kept in reserve to support frequency control. Two main methods of SOPPT

control are rotor speed control and pitch angle control. The pitch angle control is widely used for its ease of control, but is slow and increases mechanical wear and tear on the pitch system [23]. Rotor speed control does not have these drawbacks. SOPPT can be done to the left or right of the MPPT curve. If the wind turbine operates to the left of the MPPT curve, then some energy is consumed in accelerating the wind turbine to increase its output power. If it operates to the right of the MPPT curve, then energy is released into the system enhancing the frequency regulation [16].

C. Primary Frequency Controller

With power kept in reserve, the wind turbine can participate in primary frequency response. A well-established method is the power/frequency droop control method. However, this may lead to the DFIG stalling during large frequency excursions due to the significantly increased power demand. Instead, a torque/frequency droop control is suggested in [16]. The additional torque term is proportional to the frequency deviation and given by

$$\Delta T_D = k_D \left(f_{ref} - f \right) \qquad (8)$$

where k_D is the droop coefficient and f_{ref} is the nominal frequency of the system. The control system is shown in Fig. 5.
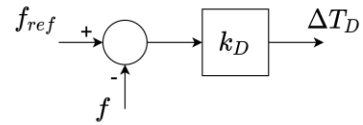

Fig. 5.   Droop controller for the wind turbine

D. Virtual Inertia

Conventional generators provide an inertial response to frequency drops by releasing kinetic energy stored in the rotating masses. A reduction in system inertia will cause larger and faster frequency deviations. Wind turbines can also provide this response through virtual inertia [5]. The idea of virtual inertia is to release stored kinetic energy in the rotating mass of the wind turbine when the frequency drops, arresting the frequency deviation and reducing the ROCOF [15]. To implement virtual inertia in the DFIG system, an additional torque term proportional to the ROCOF is included as given in [16]

$$\Delta T_H = k_H \frac{df}{dt} \qquad (9)$$

where k_H is a gain set to keep ROCOF within designated limits. A low pass filter (LPF) is included to filter out high frequency noise which can impact the derivative output [5]. The control system is shown in Fig. 6.
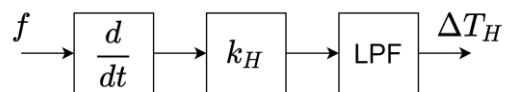

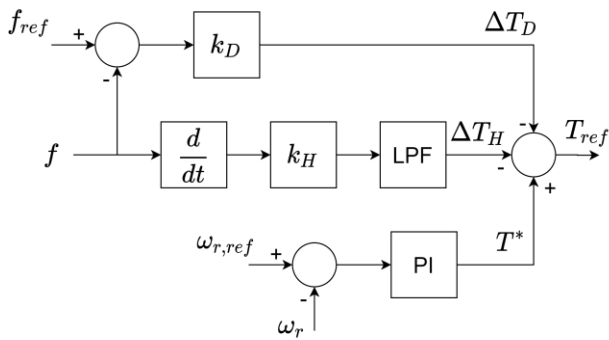Fig. 6.   Inertial controller for wind turbine

Fig. 7.   Combined controller for the wind turbine

IV. CASE STUDIES

A test isolated power system was created for the simulations. The system consists of a 3 MW diesel generator, a 1.5 MW wind turbine, and a 250 kW photovoltaic array. Five case studies are considered. In each case study, the power system is supplying an 0.8 MW load. At 40 s the solar irradiance changes from 1000 W/m^2 to 100 W/m^2 over one second. The operational frequency limits are ± 1 Hz. The goal is to minimise the frequency deviation during the under frequency event. Detailed descriptions of each case are provided below.

In the first case study (Fig. 10), the diesel generator is supplying power and the dump load is disconnected. The system configuration is shown in Fig. 8. The wind speed is 0 m/s and the wind turbine is not producing any power. At 40 s the diesel generator responds quickly to the power imbalance and increases its power output to match the generation lost. The frequency is restored to nominal quickly with a frequency nadir of 49.88 Hz (Fig. 15, blue solid line).
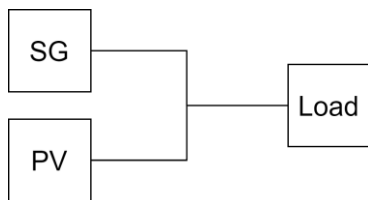

Fig. 8.   System setup for the first case study

In the rest of the case studies, the diesel engine is disconnected and the SG is converted to a synchronous condenser. A synchronous condenser (SC) can only provide reactive power and some inertia, and consumes active power to cover rotational losses [1]. It is assumed that the SC has a flywheel attached to its shaft and therefore provides greater inertia to the system. In the simulations the SC is set to consume 150 kW and uses the same excitation system to keep voltage regulated. Wind speed is increased to 11 m/s and the wind turbine now produces 1.07 MW. Therefore the system is now operating on 100% renewables. The system is depicted in Fig. 9.

In the second case study (Fig. 11), a dump load is added to the system for frequency control. The dump load will consume excess renewable generation when there is more generation
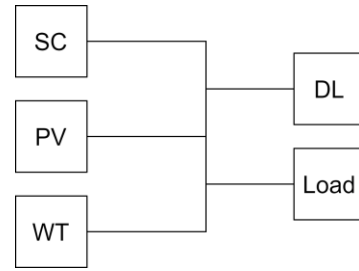

Fig. 9.   System setup for the remaining case studies

than demand to keep the frequency at the nominal value. At 40 s the dump load decreases its consumption to compensate for the lost generation. The SC has an inertial response, producing power as the rotor decelerates. The DFIG also has some inertial response without any additional control loops. The frequency nadir is 49.755 Hz (Fig. 15, orange dotted line), well within operational constraints. The dump load is able to restore frequency back to nominal, and has a frequency response comparable to the diesel generator, albeit much slower.

In the third case study (Fig. 12), the wind turbine is configured to participate in the primary frequency response using the control loop presented in Fig. 5. SOPPT is employed by running the wind turbine 0.2 pu faster than MPPT. This is not optimal but simple to implement. A droop control loop is added to the torque reference signal for primary response. The DFIG response to the under-frequency event is amplified compared to the second case. Small improvement can be seen in the frequency response from the second case, with the frequency nadir reduced to 49.780 Hz.

In the fourth case study (Fig. 13), the wind turbine is configured to provide inertial response. SOPPT is implemented in the same way as the third case. A virtual inertia control loop is added to the torque reference signal as shown in Fig. 6. The DFIG response is greater than the third case, providing more power initially but also consuming more power to return to steady state speed. A similar improvement to the third case was seen here with a frequency nadir of 49.766 Hz. This shows that in isolation the two different control loops had a similar effect on the frequency response.

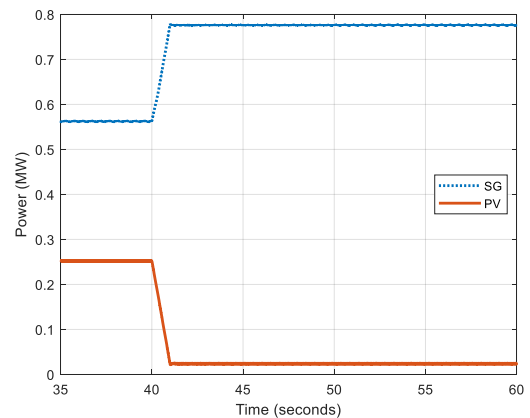In the final case study (Fig. 14), the wind turbine uses the

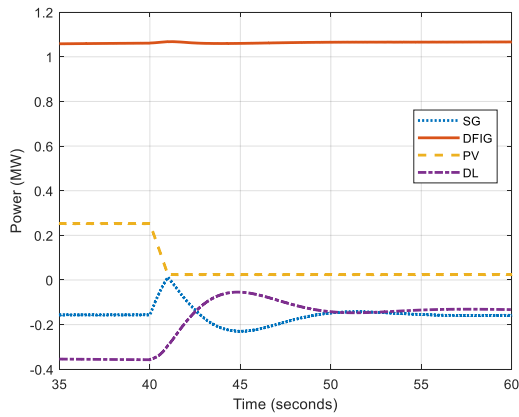Fig. 10. Case 1. Load is supplied by diesel and PV.

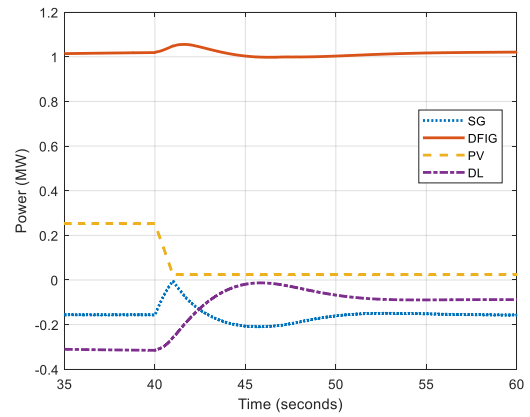Fig. 11. Case 2. Load is supplied by wind and PV. DL regulates frequency.

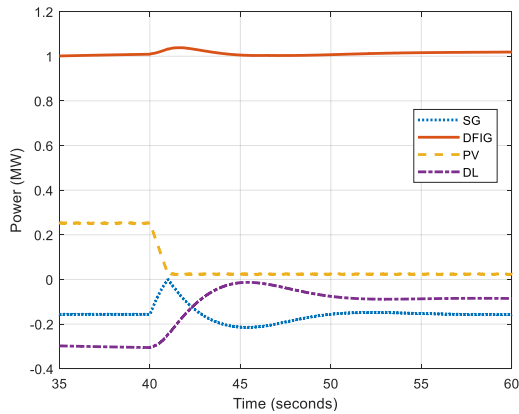Fig. 14. Case 5. Combined control is inplemented in the wind turbine.

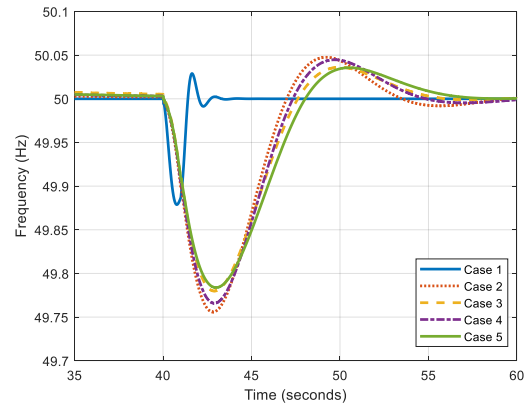Fig. 12. Case 3. Droop control is implemented in the wind turbine.

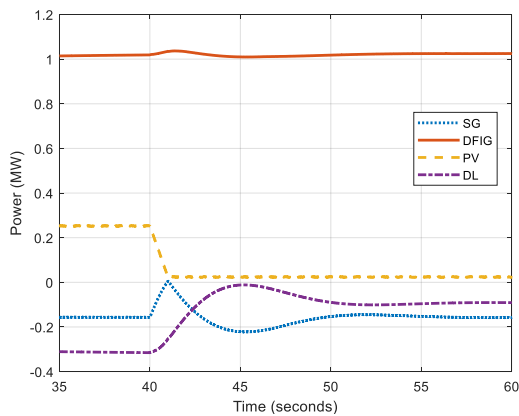Fig. 15. Frequency responses for each case study.

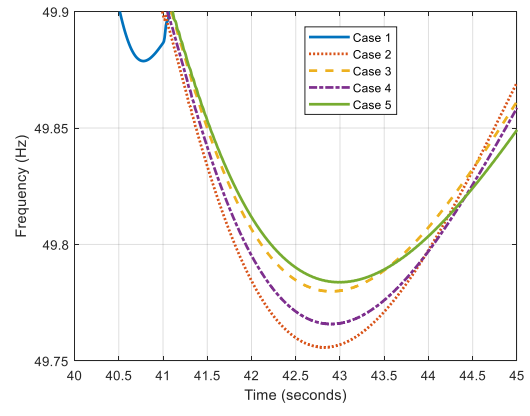Fig. 13. Case 4. Inertial control is implemented in the wind turbine.

Fig. 16. The frequency nadirs for each case study.

combined controller design provided in Fig. 7. The DFIG response is a combination of the third and fourth cases, with more power generation initially, but less power consumption to accelerate the rotor back to steady state speed. This sees the most improvement in the 100% renewable case studies with a frequency nadir of 49.784 Hz.

Fig. 16 shows the maximum frequency deviation for each case. It is clear that while the frequency deviation is decreased

with additional technology, the benefit is relatively small. This suggests that just a dump load is enough for frequency control and regulation during 100% renewable operation. The second case study with just the dump load is slower than the diesel generator but keeps frequency at nominal and has a sufficient response for normal operation.

V. Conclusion

A significant challenge facing isolated power systems is regulating frequency when the load is completely supplied by renewable energy sources. Enabling technology is required in order to achieve instantaneous 100% renewable energy penetration. Energy storage systems are a promising solution but still prohibitively expensive for many uses. A dump load is a cheap and simple technology to control frequency when there is an abundance of renewable energy generation. DFIG controls can be modified to provide enhanced frequency control by operating away from the maximum power point and using droop and inertia control. This paper has demonstrated that frequency can be controlled with diesel generation shut down without needing an energy storage system. Case studies showed that a dump load is enough for frequency regulation, and more complex control systems such as virtual inertia and suboptimal power point tracking provide minimal benefit.

References

[1] D. Nikolic and M. Negnevitsky, "Practical solution for the low inertia problem in high renewable penetration isolated power systems," in *2018 IEEE Power Energy Society General Meeting (PESGM)*, Aug. 2018, pp. 1–5.

[2] E. Semshchikov, M. Negnevitsky, J. Hamilton, and X. Wang, "Cost-efficient strategy for high renewable energy penetration in isolated power systems," *IEEE Transactions on Power Systems*, vol. 35, no. 5, pp. 3719–3728, 2020.

[3] M. O'Donovan, E. O'Callaghan, N. Barry, and J. Connell, "Implications for the rate of change of frequency on an isolated power system," in *2019 54th International Universities Power Engineering Conference (UPEC)*, 2019, pp. 1–6.

[4] G. Lalor, A. Mullane, and M. O'Malley, "Frequency control and wind turbine technologies," *IEEE Transactions on Power Systems*, vol. 20, no. 4, pp. 1905–1913, 2005.

[5] Y. Wang, G. Delille, H. Bayem, X. Guillaud, and B. Francois, "High wind power penetration in isolated power systems—assessment of wind inertial and primary frequency responses," *IEEE Transactions on Power Systems*, vol. 28, no. 3, pp. 2412–2420, 2013.

[6] C. W. Hansen and A. D. Papalexopoulos, "Operational impact and cost analysis of increasing wind generation in the island of crete," *IEEE Systems Journal*, vol. 6, no. 2, pp. 287–295, 2012.

[7] A. Oudalov, D. Chartouni, C. Ohler, and G. Linhofer, "Value analysis of battery energy storage applications in power systems," in *2006 IEEE PES Power Systems Conference and Exposition*, 2006, pp. 2206–2211.

[8] Y. Tan, K. M. Muttaqi, P. Ciufo, and L. Meegahapola, "Enhanced frequency response strategy for a pmsg-based wind energy conversion system using ultracapacitor in remote area power supply systems," *IEEE Transactions on Industry Applications*, vol. 53, no. 1, pp. 549–558, 2017.

[9] G. O. Cimuca, C. Saudemont, B. Robyns, and M. M. Radulescu, "Control and performance evaluation of a flywheel energy-storage system associated to a variable-speed wind generator," *IEEE Transactions on Industrial Electronics*, vol. 53, no. 4, pp. 1074–1085, 2006.

[10] A. Blakers, M. Stocks, B. Lu, C. Cheng, and R. Stocks, "Pathway to 100% renewable electricity," *IEEE Journal of Photovoltaics*, vol. 9, no. 6, pp. 1828–1833, 2019.

[11] F. Gutiérrez-Martín, D. Confente, and I. Guerra, "Management of variable electricity loads in wind – hydrogen systems: The case of a spanish wind farm," *International Journal of Hydrogen Energy*, vol. 35, no. 14, pp. 7329–7336, 2010.

[12] Y. Liu, W. Du, L. Xiao, H. Wang, S. Bu, and J. Cao, "Sizing a hybrid energy storage system for maintaining power balance of an isolated system with high penetration of wind generation," *IEEE Transactions on Power Systems*, vol. 31, no. 4, pp. 3267–3275, 2016.

[13] J. Hamilton, A. Tavakoli, M. Negnevitsky, and X. Wang, "Investigation of no load diesel technology in isolated power systems," in *2016 IEEE Power and Energy Society General Meeting (PESGM)*, 2016, pp. 1–5.

[14] D. Nikolic, M. Negnevitsky, and M. De Groot, "Fast demand response as spinning reserve in microgrids," in *Mediterranean Conference on Power Generation, Transmission, Distribution and Energy Conversion (MedPower 2016)*, Nov. 2016, pp. 1–5.

[15] A. Molina-García, I. Muñoz-Benavente, A. D. Hansen, and E. Gómez-Lázaro, "Demand-side contribution to primary frequency control with wind farm auxiliary control," *IEEE Transactions on Power Systems*, vol. 29, no. 5, pp. 2391–2399, 2014.

[16] Y. Tan, L. Meegahapola, and K. M. Muttaqi, "A suboptimal power-point-tracking-based primary frequency response strategy for dfigs in hybrid remote area power supply systems," *IEEE Transactions on Energy Conversion*, vol. 31, no. 1, pp. 93–105, 2016.

[17] J. Hamilton, M. Negnevitsky, X. Wang, and S. Lyden, "High penetration renewable generation within australian isolated and remote power systems," *Energy*, vol. 168, pp. 684–692, 2019.

[18] Z. Spoljaric, K. Miklosevic, and V. Jerkovic, "Synchronous generator modeling using matlab," in *28th International Conference Science in Practice (2010)*, 2010, pp. 1–6.

[19] *IEEE Recommended Practice for Excitation System Models for Power System Stability Studies*, IEEE std. 421.5, 2016.

[20] K. E. Yeager and J. R. Willis, "Modeling of emergency diesel generators in an 800 megawatt nuclear power plant," *IEEE Transactions on Energy Conversion*, vol. 8, no. 3, pp. 433–441, 1993.

[21] S. Lyden, M. E. Haque, A. Gargoom, and M. Negnevitsky, "Modelling photovoltaic cell: Issues and operational constraints," in *2012 IEEE International Conference on Power System Technology (POWERCON)*, 2012, pp. 1–6.

[22] Vinod, R. Kumar, and S. K. Singh, "Solar photovoltaic modeling and simulation: As a renewable energy solution," *Energy Reports*, vol. 4, pp. 701–712, 2018.

[23] Z. Zhang, Y. Sun, J. Lin, and G. Li, "Coordinated frequency regulation by doubly fed induction generator-based wind power plants," *IET Renewable Power Generation*, vol. 6, no. 1, pp. 38–47, 2012.